Structure and properties of the $LaCuO_{3-\delta}$ perovskites

J. F. Bringley,* B. A. Scott, S. J. La Placa, T. R. McGuire, and F. Mehran
IBM Research Division, Thomas J. Watson Research Center, Yorktown Heights, New York 10598

M. W. McElfresh
Department of Physics, Purdue University, West Lafayette, Indiana 47907

D. E. Cox
Department of Physics, Brookhaven National Laboratory, Upton, New York 11973
(Received 18 September 1992)

The high-pressure synthesis and electric and magnetic properties of the $LaCuO_{3-\delta}$ system have been studied. The copper valence can be varied in this oxygen-defect perovskite almost continuously from +3 to +2, and three distinct ordered phases are observed over its $0.0 \leq \delta \leq 0.5$ stability field. A tetragonal phase exists over the composition range $0.0 < \delta \leq 0.2$, and the structure of a sample with $\delta = 0.05$ was refined by high-resolution synchrotron powder x-ray diffraction in space group $P4/m$, with $a = 3.818\,97(4)$, $c = 3.972\,58(6)$, and $R = 0.0812$. The tetragonal phase and also a monoclinic form stable between $0.2 \leq \delta \leq 0.4$ are metallic with room-temperature resistivities of $(1.0-3.0) \times 10^{-3}$ Ω cm. The phase is orthorhombic for larger δ, becoming an insulator as $\delta \rightarrow 0.5$. Superconductivity was not observed in any of the metallic samples. Ferromagnetic behavior is observed in the tetragonal materials, but the moment disappears at the $\delta \simeq 0.2$ phase boundary. The small moment is attributed to the existence of a canted antiferromagnetic array in the tetragonal phase. The results are discussed within the contexts of schematic band models and rationalized in terms of one in which the Fermi level moves through partially overlapping copper $3d_{x^2-y^2}$ and oxygen $\pi(2p_\perp)^*$ bands as δ increases.

I. INTRODUCTION

In an earlier report,[1] we described the synthesis and general structural features of an oxygen-defect perovskite series, $LaCuO_{3-\delta}$. This phase is structurally related to the superconducting cuprates and exhibits a remarkably wide oxygen stoichiometry range, $0.0 \leq 0.5$, displaying at least three well-ordered structures. The carrier concentration can therefore be varied almost continuously from 0 to 1 hole/(Cu site) within the same basic perovskite framework. The $LaCuO_{3-\delta}$ perovskite is metallic but *not* superconductive over most of its stoichiometry range. An understanding of the normal metallic state is necessary to understand the mechanism of high-temperature superconductivity,[2] and here the normal state can be examined to very low temperatures over a wide carrier-concentration range. $LaCuO_{3-\delta}$ may also provide clues to changes in cuprate electronic structure as a function of doping, and provide a set of "standards" for the spectroscopy of Cu^{3+}, Cu^{2+} and intermediate valence states.[3,4]

The rhombohedral, high-pressure form of $LaCuO_3$ was previously prepared by Demazeau *et al.*[5] and has since been investigated by several other groups. A synthesis pressure of 65 kbar requires a high-pressure belt-type apparatus and limits the sample size to 100 mg or less. The rhombohedral phase was reported to be fully stoichiometric and to display a Pauli-like magnetic susceptibility and metallic properties down to 77 K. Webb *et al.*[6] measured the temperature-dependent susceptibility and found no evidence for a superconducting transition in rhombohedral $LaCuO_3$ above 5 K. In this paper we describe the synthesis, structural refinement, and physical properties of the tetragonal form of $LaCuO_{3-\delta}$, which exists for $0 \leq \delta \leq 0.2$, as well as our preliminary findings for the monoclinic phase at intermediate δ and the orthorhombic compound at $\delta = 0.5$. These phases are produced by a "milder" technique in which a highly reactive amorphous precursor is reacted at oxygen pressures of 0.4–1 kbar, two orders of magnitude lower than that required to prepare the rhombohedral form.[5,7]

II. EXPERIMENT

All starting materials were high-purity compounds (99.999%). Lanthanum oxide was dried and CO_2 removed by firing the powder at 950 °C prior to use. A coprecipitation technique was used to prepare the precursors to the high-pressure $LaCuO_{3-\delta}$ phases. Appropriate amounts of the binary oxides were dissolved in a slight excess of 99.9997%-purity HNO_3 by gentle heating and then diluted fivefold with deionized H_2O. The solution was then cooled to 0 °C and 99.9997%-purity NaOH was added with stirring until the solution became basic (pH $\simeq 10$) and a gelatinous blue precipitate appeared. The precipitate was filtered and washed with copious amounts of deionized H_2O to ensure that sodium had been completely removed. Elemental analyses did not reveal any sodium contamination and gave a [La]/[Cu] ratio of 0.99:1.00. The precipitate was then decomposed by slow heating to 650 °C under O_2 to yield a black, finely divided, amorphous powder. The powder was pressed into 0.5 g pellets and heated to 900 °C at oxygen pressures up to 1

kbar for 2 days.

High-pressure oxygen reactions were performed in an externally heated René alloy vessel pressurized at or below room temperature with high-purity gas (99.999%) from a standard laboratory cylinder. Reaction temperatures were measured with a thermocouple inserted in a shallow recess in the reactor wall at the sample position, and pressures were measured with an uncalibrated gauge. Samples for which $\delta \approx 0$ were obtained $P_{O_2} \gtrsim 0.5$ kbar, but in general, oxygen stoichiometries were dependent upon several factors, including the homogeneity and purity of the starting materials. Exclusion of CO_2 from the starting materials and oxidizing atmosphere was necessary to obtain the most completely reacted, homogeneously oxidized products.

Oxygen stoichiometries (δ) were established to an accuracy of ± 0.02 by reducing the samples in a thermal gravimetric analysis apparatus (TGA) under argon to $La_2CuO_4 + CuO$ (or Cu_2O), and also by electron paramagnetic resonance (EPR) spectroscopy.[3,4] The two techniques gave results in excellent agreement with each other. Figure 1(a) shows a TGA of a sample with $\delta \approx 0$. The transition marking the conversion of the tetragonal (T) to the monoclinic (M) phase at $\delta \approx 0.2$ is complete by about 400 °C. On further heating M, transforms to the orthorhombic (O) phase at $\delta \approx 0.4$ and 850 °C. The stability ranges and transition zones depend, as expected, on heating rate. the orthorhombic form at $\delta = 0.5$ could be routinely made by annealing the tetragonal form in argon at 725 °C for 16 h. On the other hand, the monoclinic phase is stable to temperatures above 800 °C at $P_{O_2} = 1$ atm [Fig. 1(b)]. By varying the temperature, time, and atmosphere, a series of T, M, and O phases with different values of δ were produced. For the tetragonal phases with $0 < \delta \leq 0.2$, annealing was carried out at temperatures below 300 °C and $P_{O_2} \leq 1$ atm. This phase is unstable toward oxygen loss even near room temperature without an oxygen overpressure, so it is not surprising that samples of fully stoichiometric $LaCuO_3$ could not be obtained, although values quite close to $\delta = 0$ were achieved.[3,4] Oxygen loss in the TGA run under argon can already be observed at the onset of heating in Fig. 1(a), while weak absorption occurs initially for the sample heated under oxygen in Fig. 1(b).

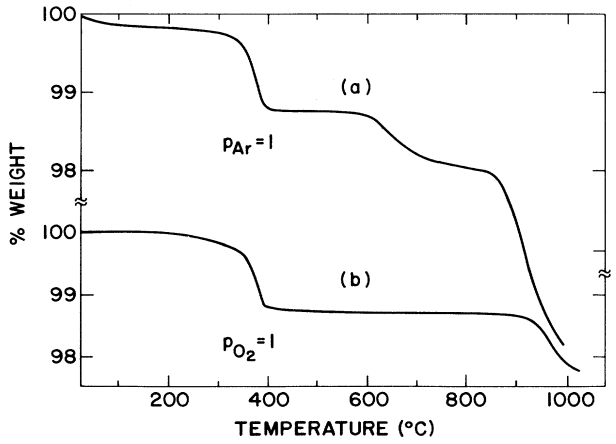

FIG. 1. Thermal gravimetric analysis of $LaCuO_{3-\delta}$ for $\delta \approx 0$. (a) Argon atmosphere. (b) Oxygen atmosphere.

High-resolution synchrotron x-ray powder-diffraction data were collected at beamline X7A of the Brookhaven National Synchrotron Light Source. A sample of composition $LaCuO_{2.95}$ was mounted in the flat plate geometry. A monochromatic beam of wavelength 1.2015 Å was obtained using a channel-cut Si(111) monochromator scattering in the vertical plane and a Ge (220) analyzer. Data were collected at 0.005° (2θ) intervals over the angular range 10°–90°. The sample was rocked at each point to obtain a proper powder average over the crystallites. Temperature-dependent data were collected using a closed cycle helium refrigerator equipped with Be windows. Step scans were carried out over selected angular regions containing the (101), (110), (111), (002) and (200/020) reflections at temperatures of 300, 270, 180, and 18 K. Thermal-expansion coefficients were determined from lattice parameters refined from these reflections. Structural refinements were performed using a modified version of the Rietveld program.[8] Forty-seven independent Bragg intensities were used in the refinement; very weak intensities attributed to La_2CuO_4, $LaCuO_{2.6}$ (M), and CuO were excluded from the refinement. Nineteen parameters were refined including cell parameters, atomic positional, and anisotropic thermal parameters, overall scale factor, peak shape functions, and zero-point error.

Temperature-dependent electrical resistivity measurements were performed on rectangular bar-shaped tetragonal phase specimens cut from pellets sintered at 925 °C at various oxygen pressures. A sintering time of several days was necessary to obtain suitable samples. Monoclinic and orthorhombic samples were prepared from these bars using procedures discussed above. The specimens were about 0.5 mm by 1.0 mm in cross section and the current density ranged from about 50–100 mA/cm^2. A standard four-probe ac lock-in technique was used and contacts were made with spring loaded pins. Magnetic susceptibility measurements were performed on a Quantum Design superconducting quantum interference device magnetometer over the temperature range of 5–300 K in fields up to 55 kOe.

III. RESULTS AND DISCUSSION

A. Structural refinement

The structure of the tetragonal phase was refined from the high-intensity powder data in space group $P4/m$. Initial refinements allowing only isotropic thermal motion with fixed positional parameters resulted in anomalously large thermal parameters for oxygen. Subsequent refinements were then performed, firstly, allowing for anisotropic thermal vibration, and secondly, isotropic thermal motion allowing a static disorder of oxygen off their ideal positions. The observed and difference powder-diffraction profiles of the later model of $LaCuO_{2.95}$ are shown in Fig. 2. The structure of the tetrag-

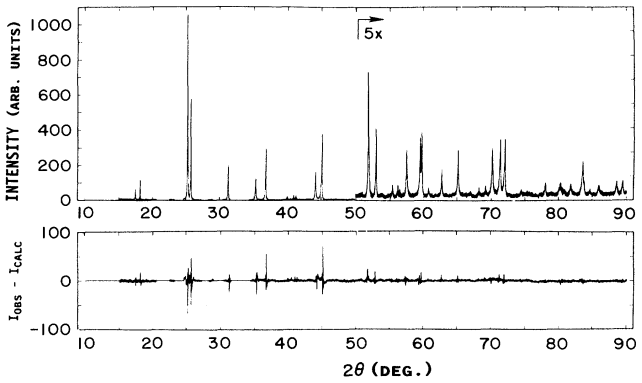

FIG. 2. The observed, calculated, and difference profiles of $LaCuO_{2.95}$ at room temperature. The region between $2\theta = 40-90°$ is shown on an expanded scale for clarity.

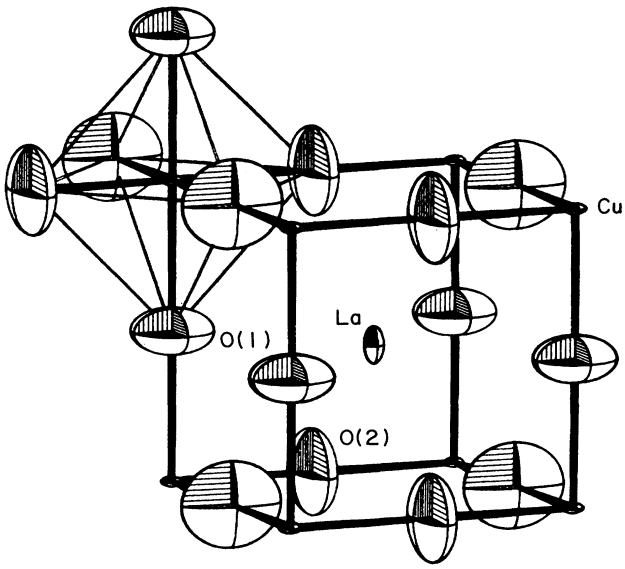

FIG. 3. The structure of $LaCuO_{2.95}$ illustrating the anisotropic thermal parameters of oxygen. The unit cell is outlined and the octahedral coordination of copper is emphasized. Atoms shown are 50% probability ellipsoids.

onal phase at composition $LaCuO_{2.95}$ is shown in Fig. 3. The refined atomic positions, occupancies and anisotropic thermal parameters are given in Table I. The structure consists of a simple tetragonal distortion of a cubic perovskite and $a = 3.818\,97(4)$ Å and $c = 3.972\,58(6)$ Å. There are four La-O(1) distances of 2.700 Å and eight La-O(2) at 2.755 Å. The distortion is brought about by a slight Jahn-Teller-like elongation of the CuO_6 octahedra, in which there are four in-plane Cu-O bonds at 1.909 Å, and two apical Cu-O bonds at 1.986 Å. This is in contrast to the rhombohedral form in which all Cu-O distances are equal at 1.94 Å.[5] The anisotropic thermal parameters indicate a vibration of the oxygen atoms perpendicular to the metal-oxygen bond, and is reminiscent of that observed in the closely related compound $Ba_{0.87}K_{0.13}BiO_3$.[9] This vibrational motion is tantamount to a tilting distortion of the CuO_6 octahedra. Alternatively, allowing a static disorder of oxygen off the ideal positions, $(0,0,\frac{1}{2})$, and $(0,\frac{1}{2},0)$ results in improved isotropic thermal parameters, $B_{iso} = 1.8(3)$ and 2.3(5) for O(1) and O(2), respectively, and improved occupational factors (Table I b). The magnitude of the disorder corresponds to a displacement of oxygen by about 0.41 Å and refinement yielded a convergence to the final agreement factors $R = 8.12\%$, $R_p = 13.83\%$, and $R_{wp} = 19.05\%$. The statistically expected R factor, R_{exp} was 12.71% leading to a goodness of fit, $S_p^2 = (R_{wp}/R_{exp})^2 = 2.25$. R values and goodness of fit are defined elsewhere.[10] The thermal-expansion coefficients measured between 11 and 300 K for the tetragonal form are $\alpha_a = 3.5 \times 10^{-5}$ Å/K and $\alpha_c = 1.4 \times 10^{-5}$ Å/K.

The unit-cell volume of the tetragonal phase (57.993 $Å^3$) is only slightly larger than that of the rhombohedral form (57.721 $Å^3$), consistent with the latter being the high-pressure dimorph of $LaCuO_3$. Tetragonal $LaCuO_3$ has also been prepared by the method of Darracq, *et al.*

TABLE I. Crystallographic data of $LaCuO_3$ tetragonal cell, space group $C_{4h}^1 - P_{4/m}$ (No. 83), $Z = 1$ $a = 3.818\,97(4)$ Å, $c = 3.972\,58(6)$ Å, Vol = 57.993(2) $Å^3$, and $d_{calc} = 7.178$ g/cm^3. The anisotropic thermal parameters are of the form $\exp-[\beta_{11}h^2+\beta_{22}k^2+\beta_{33}l^2+2\beta_{12}hk+2\beta_{13}hl+2\beta_{23}kl]$. $\beta_{13} = \beta_{23} = 0$.

(a)

Atom	Position	x	y	z	β_{11}	β_{22}	β_{33}	β_{12}
Cu	1*A*	0	0	0	0.0086(7)	0.0086(7)	−0.002(1)	0.0
La	1*d*	$\frac{1}{2}$	$\frac{1}{2}$	$\frac{1}{2}$	0.0083(4)	0.0083(4)	0.0291(8)	0.0
O(1)	1*b*	0	0	$\frac{1}{2}$	0.151(11)	0.151(11)	0.047(10)	0.00
O(2)	2*e*	$\frac{1}{2}$	0	0	0.036(8)	0.24(1)	0.17(1)	0.017(9)

(b)

Atom	Position	x	y	z	B ($Å^2$)
Cu	1*a*	0	0	0	0.63
La	1*d*	$\frac{1}{2}$	$\frac{1}{2}$	$\frac{1}{2}$	0.75
O(1)	8*l*	0.500	0.085(2)	0.060(2)	1.79
O(2)	4*k*	0.093(5)	0.000	0.500	2.35

in a belt-type apparatus at 20 kbar, in a series of experiments which confirmed it to be the low-pressure form.[7] Webb *et al.*[6] report a tetragonal phase of $LaCuO_3$ with lattice parameters $a = 5.431$ Å and $c = 7.84$ Å, obtained by heating the rhombohedral form to 408 °C. However, not all reflections in the powder pattern of this material could be indexed, and there was generally a poor fit between the observed and calculated powder patterns. Furthermore, no attempt was made to measure the oxygen content and it seems likely that this material may be nonstoichiometric, possibly related to the phases with $\delta > 0.2$ which we have previously reported.[1] Comparison of the diffraction pattern[6] with that of the tetragonal phase reported herein did not reveal any obvious similarities. The detailed structures of the monoclinic ($\delta = 0.2$–0.4) and orthorhombic ($\delta = 0.4$–0.5) forms have been discussed elsewhere.[1,11,12]

B. Transport and magnetic measurements

The electrical resistivities for tetragonal phase materials having oxygen contents of $\delta \simeq 0$, 0.09, and 0.16, and a monoclinic sample with $\delta = 0.33$, are shown in Fig. 4 as a function of temperature. Data for the $\delta = 0.5$ phase are not presented, as this material was found to be insulating, with $\rho > 10^6$ Ω cm at room temperature. Results for superconducting $YBa_2Cu_3O_7$ are also shown in Fig. 4 for comparison.

The temperature dependences of all the samples clearly indicate metallic behavior. The room-temperature resistivities range from 1.0–3.0 mΩ cm, only slightly higher than sintered ceramic specimens of the metallic, superconducting cuprates. These values, however, are still very large for metals, suggesting a considerable disorder scattering contribution. The residual resistivities (ρ_R) increase with δ, ranging from 0.4 mΩ cm for $\delta \approx 0$ to 0.8 mΩ cm for $\delta = 0.33$. The increase in ρ_R with δ is consistent with an increase in the scattering associated with the lattice defect concentration. If we assume a linear temperature dependence for the $LaCuO_{3-\delta}$ samples at higher temperatures, the slopes ($d\rho/dT$) range from 2.0–4.0 μΩ cm K^{-1}. As is apparent from Fig. 4, no superconducting transition was found in any of these samples above 5 K. In addition, no evidence for superconductivity was found in resistivity measurements of the $\delta \approx 0$ and $\delta = 0.11$ samples down to 0.5 K.

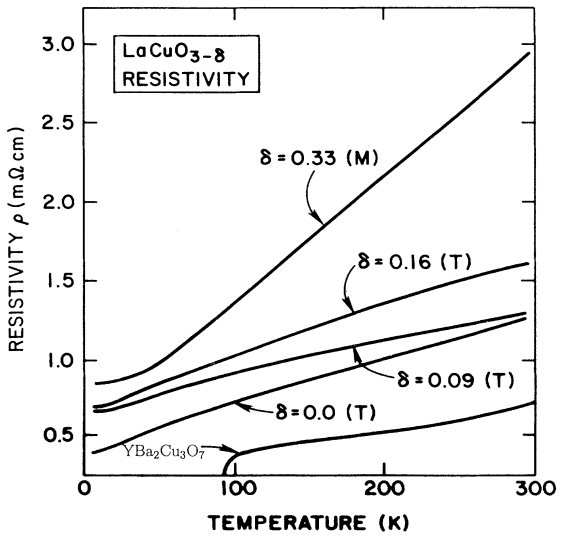

FIG. 4. Resistivity vs temperature for sintered specimens of $LaCuO_{3-\delta}$. Data for $YBa_2Cu_3O_7$ are shown for comparison.

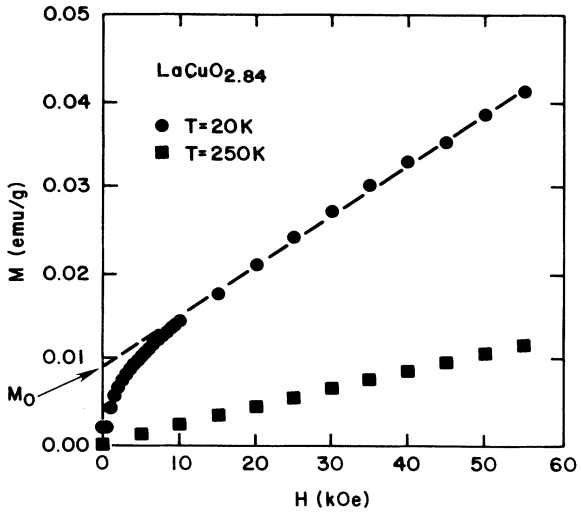

FIG. 5. M vs H at 20 and 250 K for tetragonal $LaCuO_{2.84}$.

Magnetization data are illustrated in Figs. 5, 6, and 7. The M vs H plots in Fig. 5 for $LaCuO_{2.84}$ at 20 and 250 K show that there is a weak ferromagnetic behavior at lower temperatures. We obtain the ferromagnetic component M_0 by projecting the high-field slope to $H = 0$ as indicated by the dashed line in Fig. 5. Figure 6 shows M_0 as a function of temperature for several compositions. The paramagnetic susceptibilities shown in Fig. 7 were obtained from the high-field slopes of the M vs H plots at each temperature.

Consider initially the ferromagnetic contribution M_0 in Fig. 6 which has values from 2 to 10 emu/mol at 4.2 K. We believe this is an intrinsic moment and not due to an

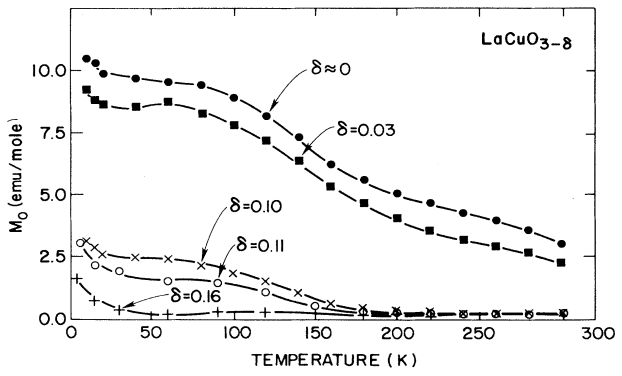

FIG. 6. The temperature dependence of the ferromagnetic moment (M_0) for several compositions of $LaCuO_{3-\delta}$.

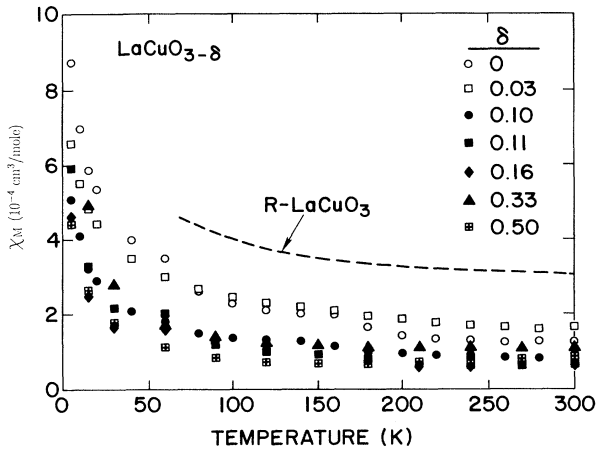

FIG. 7. Temperature dependence of the molar magnetic susceptibilities for several tetragonal, monoclinic, and orthorhombic $LaCuO_{3-\delta}$ samples. The results for rhombohedral $LaCuO_3$ were taken from Ref. 5.

impurity phase for the following reasons. First, the most likely impurities are small amounts of La_2CuO_4, CuO, or even trace quantities of the monoclinic form ($\delta=0.2$–0.4). However, the two former materials are antiferromagnetic, while the latter is nonmagnetic. Further, it is seen that M_0 changes with the oxygen-defect concentration δ, declining from 10 emu/mol for $\delta\approx 0$, to $M_0\approx 0$ at the tetragonal-to-monoclinic phase boundary at $\delta\approx 0.2$. Finally, there is very strong EPR and magnetic evidence that the highly diluted Cu^{2+} cations in the phases with $\delta\approx 0$ interact ferromagnetically at long range and undergo a phase transition at temperatures below 240 K.[3,4] The fact that the temperature dependence of the EPR parameters are δ dependent is particularly compelling. For these reasons, we believe that the small moments observed are intrinsic and the data are analyzed under this assumption.

Figure 7 shows the temperature dependence of the molar susceptibility (χ_M) for the sequence of samples given in Fig. 6, but also including monoclinic ($\delta=0.33$) and orthorhombic ($\delta=0.5$) phases. The data of Fig. 7 can be approximately fit to a Curie-Weiss law plus a temperature-independent susceptibility (χ_0) of the form $\chi_M=\chi_0+C_M/(T-\Theta)$. Weiss constants are very small, $\Theta<\pm 20$ K, and $\chi_0\approx 10\times 10^{-5}$ cm^3/mole over the composition fields of the *T*, *M*, and *O* phases. The Curie constant is $C_M\approx 14\times 10^{-3}$ for $\delta\approx 0$ and 0.03, declining to $C_M\approx 6\times 10^{-3}$ cm^3 K/mole for $\delta=0.12$ to 0.5. Theory for Cu^{2+} with one unpaired spin gives $C_M=0.375$ and we assume Cu^{3+} is in a low spin state with $C_M=0$. Thus, the measured values of C_M are only a few percent of the number of Cu^{2+} as given by δ.

IV. DISCUSSION

Copper in $LaCuO_3$ is formally Cu^{3+}, a d^8 cation, and its low spin state ($S=0$) is the one most commonly observed in octahedral crystal-field environments. As δ increases a corresponding fraction of the Cu formally become Cu^{2+}, a d^9 cation with $S=\frac{1}{2}$. For example, at the composition $\delta=0.16$ there would be 0.32 Cu^{2+} ions per mole of $LaCuO_{2.84}$. Taking $C_M=0.006$, as given above, no more than 4% of the expected number of Cu^{2+} cations are actually contributing to C_M. In addition to the anticipated increase in Curie component with δ (which is not observed), changes in χ_0 should also occur due to an increase in the Pauli susceptibility with carrier concentration. The actual results, showing no clear trend in χ_0, of course are contrary to these expectations. Given the observation of a small ferromagnetic moment in the tetragonal phase, the susceptibility results of Fig. 7 can not be used as a guide to a magnetic model for the tetragonal phase. In fact, in large part the data more likely reflect, especially at the lowest temperatures studied, actual paramagnetic impurities present in all the compositions of the $LaCuO_{3-\delta}$ system.

Although we believe that the weak ferromagnetism of the tetragonal phase is intrinsic, the value $M_0\simeq 10$ emu/mole obtained at low temperature for $\delta\approx 0$ is quite small, corresponding to 0.2% Cu^{2+}. This concentration is obtained from the fact that a full ferromagnetic moment of $1\mu_B$ for Cu^{2+} corresponds to $M_0=5586$ emu/mole, and this is consistent with EPR intensity measurements.[3] Moreover, the moment should disappear entirely at $\delta=0$. Consistent with this expectation, Darracq, Matar, and Demazeau[13] have prepared a tetragonal $LaCuO_3$ at 40 kbar, and it shows no evidence for magnetic ordering at low temperatures. Unlike our material, produced at oxygen pressures below 1 kbar, the composition of the phase of Darracq, Matar, and Demazeau is probably very close to $\delta=0$. The magnetic measurements for the "$\delta\approx 0$" sample shown in Fig. 6 suggest, in fact, that its actual composition is closer to $\delta\approx 0.001$.[4]

If the observed moments are not due to contamination by impurities, as we believe, then their small values at lower temperatures in the tetragonal (*T*) phases with $\delta>0$ could arise from antiferromagnetic ordering with a canting of the spins off the spin axis. The canting would produce a small ferromagnetic component that saturates at low field. As the oxygen defect concentration δ increases, more Cu^{2+} are created, but antiferromagnetic correlations become very strong and decrease both M_0 and possibly also χ_M as illustrated in Figs. 6 and 7. In addition, there is likely to be considerable covalent mixing of Cu and O wave functions, leading to a large reduction in p_{eff}. Thus, there would be little evidence for localized Cu^{2+} cations in these highly correlated yet still delocalized metallic systems.

In a cubic perovskite the crystal fields split the fivefold orbital degeneracy of the *d* states into a lower triplet (t_{2g}) and upper doublet (e_g). The latter in turn is split into d_{z^2} and $d_{x^2-y^2}$ singlets by tetragonal or lower (orthorhombic, monoclinic, but not trigonal) distortions, with the $d_{x^2-y^2}$ state highest for an elongation of the bonds along the symmetry axis, as in *T*-$LaCuO_3$. The lower t_{2g} states break up into a doublet and a singlet by either a trigonal or a tetragonal distortion, but in the cuprates they are occupied and do not influence the physical properties. As

discussed by Goodenough *et al.*,[14] R-$LaCuO_3$ should be metallic since the two e_g electrons per Cu^{3+} (d^8) are in an orbitally degenerate state that would broaden into a half-filled band. On the other hand, if the correlations are large compared to the bandwidths, the rhombohedral phase would be insulating because of the presence of a Hubbard gap (U). For the tetragonal phase, if bandwidths are small compared to the crystal-field splitting, T-$LaCuO_{3-\delta}$ with $\delta \approx 0$ should be an insulator, since the $d_{x^2-y^2}$ band is empty and the d_{z^2} band is full. What is observed, of course, is that both R- and T-$LaCuO_3$ are poor metals. This suggests that the bandwidths are large enough for some overlap to occur between empty and full Hubbard bands in the rhombohedral case, and between the empty $d_{x^2-y^2}$ and full d_{z^2} bands in the tetragonal form. For the latter, this oversimplified situation is depicted in the schematic $3d$-band model of Fig. 8, which also shows how the Fermi level moves through the T, M, and O phases with increasing δ, leading to a Hubbard gap at $\delta = 0.5$.

The nature of the magnetic correlations in the two high-pressure forms of $LaCuO_3$ are likely to be very different. In the rhombohedral case, since the states originate from half-filled bands, the correlations would be antiferromagnetic.[15] In the tetragonal and lower symmetry cases, since the conduction electrons are in originally empty states, the correlations could be ferromagnetic.[16] As δ increases through the stability fields of the $LaCuO_{3-\delta}$ phases, oxygen vacancies are created which act as double donors, increasing the Fermi level so that at $\delta = 0.5$ the $d_{x^2-y^2}$ band would become half filled. In a system with strong correlations, the resulting Hubbard gap would make $LaCuO_{2.5}$ an insulator, as observed. As the oxygen content decreases through the T, M, and O phases, magnetic correlations shift from ferromagnetic to antiferromagnetic, with an intervening antisymmetric (canted) state. Both magnetic susceptibility and EPR (Refs. 3 and 4) are consistent with the presence of a small ferromagnetic moment for a small but nonzero δ. As the ferromagnetic interaction diminishes with increasing δ, EPR linewidths increase because of antisymmetric and antiferromagnetic correlations which ultimately produce

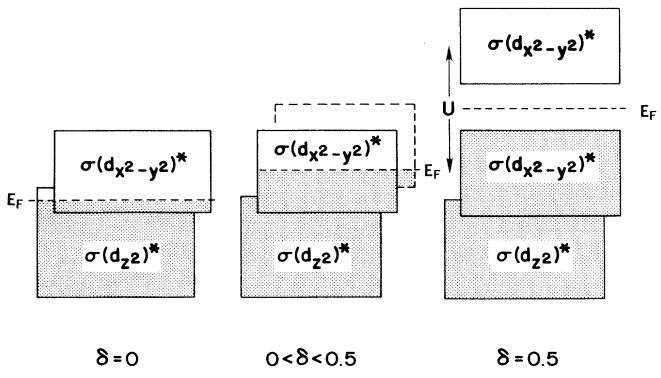

FIG. 8. Schematic d-band model for $LaCuO_{3-\delta}$ showing metallic conductivity arising from the overlap of $3d$-like σ^* subbands.

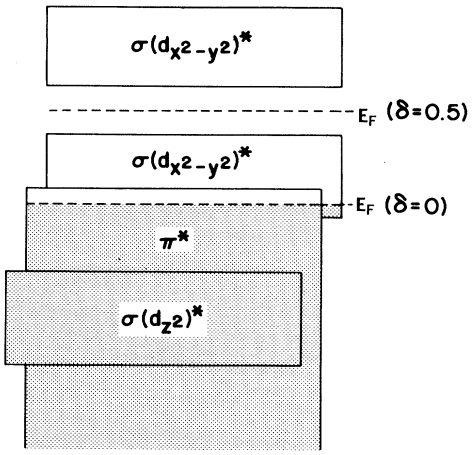

FIG. 9. Schematic band model for $LaCuO_{3-\delta}$ showing metallic conductivity arising from the overlap of σ^* and π^* subbands.

the Hubbard insulator at $\delta = 0.5$. Finally, we point out that Anderson magnetic localization[17] provides a similar context to explain the evolution of magnetic properties. In this picture, as δ increases, spinless Cu^{3+} cations become Cu^{2+} with spin $\frac{1}{2}$, which localize in the background of band states. For small δ, these localized Cu^{2+} centers interact ferromagnetically at long range. At the other extreme, $\delta = 0.5$, the system would evolve into a concentrated Anderson lattice of Cu^{2+} centers, giving rise to an antiferromagnetic insulator, with canted magnetism observed at intermediate δ. More detailed magnetic measurements including neutron diffraction are required to obtain a complete and credible model. The full picture requires an understanding of the influence of the various oxygen defect structures on the magnetic properties of the entire $LaCuO_{3-\delta}$ system.

A more realistic band scheme than that depicted in Fig. 8 is implied by our EPR results.[3,4] The EPR spectra show $g_\perp \lesssim 2$ for tetragonal phases with $\delta \approx 0$. Analysis of the data suggests that the anomalously low $g_\perp$ could be explained by the presence of oxygen $\pi(2p_\perp)^*$ states at E_F.[18] This would lead to a band model such as that shown in Fig. 9, where metallic character for $\delta \approx 0$ occurs as a consequence of the overlap of the empty $\sigma(d_{x^2-y^2})^*$ band with the filled π^*. Such a picture is consistent with band-structure calculations by Darracq, Matar, and Demazeau,[13] and the view of $LaCuO_3$ as a "low-Δ" metal.[19] A perplexing experimental issue, however, is the finding of semiconducting behavior for the presumably fully stoichiometric T-$LaCuO_3$ phase.[13] In Fig. 9, the transformation of $LaCuO_{3-\delta}$ to an insulator as $\delta \rightarrow 0.5$ arises from the same mechanism as that shown for the simple d-band case of Fig. 8; namely, the development of a Hubbard gap as the $\sigma(d_{x^2-y^2})^*$ band becomes half filled at $LaCuO_{2.5}$

ACKNOWLEDGMENTS

The authors wish to thank Richard F. Boehme for assistance in collecting diffraction data, P. Santhanam for

his help with the low-temperature resistivity measurements, and Steve Trail for assistance with sample preparations. We are also grateful to Tom Shaw, Jerry Torrance, and Al Overhauser for valuable discussions, and to Professor G. Demazeau for communicating Ref. 13 prior to publication. M.W.M. was supported in part by the Midwest Superconductivity Consortium through DOE Grant No. DE-FG02-90ER45427 and D.E.C. by the U.S. Department of Energy, Division of Materials Sciences under Contract No. DE-AE02-76CH00016.

---

*Present address: Eastman Kodak Company, Health Sciences Division, Bldg. 81, 7th Floor, Rochester, NY 14650-2033.

[1]J. F. Bringley, B. A. Scott, S. J. La Placa, R. F. Boehme, T. M. Shaw, M. W. McElfresh, S. S. Trail, and D. E. Cox, Nature (London) **347**, 263 (1990).

[2]K. Levin, J. H. Kim, J. P. Lu, and Q. Si, Physica C **175**, 449 (1991).

[3]F. Mehran, T. R. McGuire, J. R. Bringley, and B. A. Scott, Phys. Rev. B **43**, 11 411 (1991).

[4]F. Mehran, T. R. McGuire, J. F. Bringley, and B. A. Scott, J. Magn. Magn. Mater. **104-107**, 637 (1992).

[5]G. Demazeau, C. Parent, M. Pouchard, and P. Hagenmuller, Mater. Res. Bull. **7**, 913 (1972).

[6]A. W. Webb *et al.*, Phys. Lett. A **137**, 205 (1989); Physica C **162**, 899 (1989).

[7]S. Darracq, A. Largeteau, G. Demazeau, B. A. Scott, and J. F. Bringley, Eur. J. Solid State Inorg. Chem. **29**, 585 (1992).

[8]H. M. Rietveld, J. Appl. Cryst. **2**, 65 (1969).

[9]J. P. Wignacourt, J. S. Swinnea, H. Steinfink, and J. B. Goodenough, Appl. Phys. Lett. **53**, 1753 (1988).

[10]J. P. Attfield, A. K. Cheetham, D. E. Cox, and A. W. Sleight, J. Appl. Cryst. **21**, 452 (1988).

[11]S. La Placa, J. F. Bringley, B. A. Scott, and D. E. Cox, Acta Crystallogr. (to be published).

[12]S. La Placa, J. Bringley, R. Boehme, D. Cox, and B. Scott (unpublished).

[13]S. Darracq, S. Matar, and G. Demazeau (unpublished).

[14]J. Goodenough, N. F. Mott, M. Pouchard, G. Demazeau, and P. Hagenmuller, Mater. Res. Bull. **8**, 647 (1973).

[15]W. F. Brinkman and T. M. Rice, Phys. Rev. B **2**, 4302 (1970).

[16]D. M. Edwards and E. P. Wohlfarth, Proc. R. Soc. London Ser. A **303**, 127 (1968).

[17]P. W. Anderson, Phys. Rev. **124**, 41 (1961).

[18]F. Mehran (unpublished).

[19]J. B. Torrance, P. LaCorre, C. Asavaroengchai, and R. M. Metzger, J. Solid State Chem **90**, 168 (1991).